Hindawi
International Journal of Antennas and Propagation
Volume 2023, Article ID 8602885, 14 pages
https://doi.org/10.1155/2023/8602885

Research Article

Real-Time Implementation of a Novel Design Approach for Sub-GHz Long-Range Antenna for Smart Internet of Things Communication

Sneha Bhardwaj,[1] **Praveen Kumar Malik**,[1] **Anish Gupta**,[2] **and Rajesh Singh**[3]

[1]*School of Electronics and Electrical Engineering, Lovely Professional University, Jalandhar, Punjab, India*
[2]*Apex Institute of Technology, Chandigarh University, Punjab, India*
[3]*Division of Research and Innovation, Uttaranchal University, Dehradun, Uttarakhand 248007, India*

Correspondence should be addressed to Praveen Kumar Malik; praveen.23314@lpu.co.in

Received 29 June 2022; Revised 16 September 2023; Accepted 29 September 2023; Published 16 October 2023

Academic Editor: Arpan Desai

This research article designs and develops a planar small-size antenna design for smart Internet of Things (IoT) communication with long-range technology (LoRa). The proposed system is best suited for transceiver systems in this automation and sensing era. In the proposed antenna, the ground, the radiating element, and the stub feed are designed on the same side of the substrate, keeping in mind that it can print the LoRa module. The design consists of a meandered monopole, a dipole structure as a ground, and a stub feed. A different design approach is employed to get an optimized result. The antenna is made up of a rectangular feed stub to which a connecting wire is attached. The overall dimension of the antenna is 55 m × 55 m × 1.6 mm. To verify the proposed design, an antenna was fabricated and measured, which covers the LoRa frequency band at 868 MHz, providing a sufficient bandwidth of 10 MHz and a gain of more than 0.5 dB in the operating band. A designed antenna is implemented for sensor data communication with the LoRa module device and device interface Arduino platform. The antenna is connected as a transmitter and receiver one by one to verify its performance with machine-to-machine communication using the LoRa module. The size, bandwidth, and radiation efficiency of this antenna are better than the antennas in the literature. The designed antenna is successfully implemented with LoRa connectivity and communicates the data up to 8 km in line-of-sight communication, more than 1 km in urban environments, and approximately 250 m of connectivity in building areas.

1. Introduction

Long-range technology is a wireless technology developed to meet the requirements for longer coverage, low-power devices, and deep indoor penetration. Overall, this technology is a boon for the IoT era because it helps to increase network coverage, battery life, and spectrum efficiency of devices. Because the LoRa device can communicate with the LoRa module through its interface, it does not require a network for connectivity. As a result, LoRa is beneficial for rural, forest, and mountain areas to track nature where there is no Internet network. LoRa technology is in high demand for monitoring, tracking, and sensing [1]. These characteristics of LoRa allow it to be used in a variety of applications, as shown in Figure 1 [2]. However, as shown in Figure 1, there are some applications, where very small data must be communicated, as in sensor data communication. For example, temperature and humidity sensors are used in smart agriculture; light and gas detector sensors are used in smart homes; light sensors are used in smart street lighting systems and location tracking systems; bin full sensors are used in waste management systems; vacant space sensors are used in smart parking systems; and many more sensors' data are used for automation.

In India, the LoRa communication spectrum is 865.867 MHz [3]. The LoRa frequency in Europe is 868 MHz, while in the United States, it is 915 MHz, with a bandwidth of 125 kHz for both up and down frequencies. LoRa technology

Figure 1: Different fields where the LoRa can play a major role in sensor data communication [2].

makes it possible to talk over long distances while using very little power. This fills a traditional gap in sensor networks. It also works well with other technologies because it operates in an unlicensed band and is suited for both indoor and outdoor use. Because LoRa is based on the open-source Lora WAN protocol, it is a globally accessible network [4]. Sensors, boards, the processing unit, the LoRa module (Arduino), and antennas are all included in the smart devices. Several sensors are used in automation and smart communication for data collection, processing, and management. Because there is no generally established standard for smart long-range communication, it is a chance to adapt and modify existing high-accuracy protocols, such as SIGFOX and LoRa, which are also used by the industry for long-range communication [5]. However, Wi-Fi is another commonly used standard for smart communication. It consumes a lot of power and has a maximum coverage range of 40–45 m, so long-range communication and Wi-Fi interbuilding are not possible. So, the antenna design focuses on miniaturization without reducing the size of smart sensors. This makes it possible to build a small, compact device that can use LoRa technology to transfer data while using very little power.

Various issues with IoT antennas used for different frequencies are discussed in the literature, with some focusing on tiny and low-profile antennas. Table 1 compares the suggested design to their prototype to validate the benefits of the designed antenna in terms of performance, size, bandwidth, and design complexity. The monopole antenna is shown in [17–19] for wideband applications. In the literature, some meandering antennas are designed for IoT applications [20]. In [21, 22], slots, slits, and inductive loading with vias achieve more than 90% miniaturization, and the design is usable in the 805–835 MHz frequency range. Most PIFA antennas are conceived and developed for L-band communication. Because it can operate digitally and provide low-power communications, the PIFA structure is a viable choice for sub-GHz range applications. Folded dipole approaches and meandering techniques are used to reduce size [23–25], and meander line antennas outperform PIFA in terms of bandwidth and radiation efficiency [26, 27]. In some literature, the metamaterial concept is also used to reduce the size of an antenna, increase the bandwidth of an antenna, and improve the radiation of an antenna [6, 28]. The metamaterial concept is useful in creating a compact antenna, but design complexity is also increased as compared to the monopole design [29]. The surface waves always play a role in the gain and efficiency of the antenna. The surface reduction techniques are also studied and taken into account as per the literature [30]. Only one type of monopole antenna, the meander line antenna, gives good efficiency with moderate sensitivity [31]. So, the meandering approach to building a small antenna for LoRa communication is sorted after all references.

In this article, a meandered monopole antenna is designed which has a dipole-shaped ground, and feed is given by a rectangular stub between the ground and patch. The proposed design can be operated for LoRa applications in the 868 MHz spectrum. The antenna is designed and fabricated on a flame retardant (FR4) substrate with $\varepsilon_r = 4.4$. The designed antenna is fabricated and measurements are taken to cross-check the results with the simulated one.

The novelty of the proposed work can be summarised as follows:

(1) To overcome the issues of coverage for LoRa devices, the proposed antenna has better coverage than the previously designed antenna and conventional monopole antenna. The proposed antenna meets the requirements for LoRa communication.

(2) The design is also simple, so there is ease of fabrication and the small-size tends to the placement of this antenna at the LoRa module, which will decrease the size of the communication module of the LoRa device.

(3) A compact meandered antenna is proposed for LoRa applications. The work cited in [31–35] covered the *L* bands, but they are not suitable for LoRa communication.

(4) While optimizing the size of the antenna, a unique meandered design is implemented with the dipole-shaped ground. As per the author's information, such a unique design with a compact size, low cost, and good gain is not achieved in any work.

The proposed antenna design techniques, strategy, and theoretical analysis are discussed in Section 2, and the simulated and measured results are mentioned in Section 3. Section 4 deals with the real-time implementation of the LoRa antenna in different environments. In Section 5, the article is concluded.

Table 1: Comparison of the proposed antenna with other antennas published in recent years.

Reference	Design technology	Dimension (mm^2)	Substrate	Frequency	Bandwidth (MHz)	Design complexities	Gain (dB)
[6]	Meandered technology and folded	125 × 103	FR4	410 MHz	40	Design is complex as via is present	−6
[7]	PIFA design	91 × 69	PCB	868 MHz	20	Simple design	NA
[8]	Slot technique	105 × 82	FR4	433 MHz	6	Simple design with slot must be optimized	2.19
[9]	UCA design	100 × 35	FR4	868 MHz	2	Trade design cannot be used universally	−4.3
[10]	H-shaped, slotted monopole with diode tuning	60 × 27	RO-4350	868	10	Design is very complex as the diode tuning and via are present	0.96
[11]	Bow-shaped patch antenna and DGS	120 × 70	FR4	868 MHz	23	Simple design	NA
[12]	Metamaterial concept, CSRR	25 × 25	FR4	912 MHz	60	Design is complex	NA
[13]	Flexible textile, wearable antenna, dipole	150 × 110	Silver ink sheet	868 MHz	32	Design is complex	NA
[14]	Flexible substrate meandered design	85 × 169	Textile	433 MHz	30	Simple design	1.25
[15]	Power divider feed and slotted patch	90 × 90	RF35	2.4 GHz	100	Design is complex as a power divider and via is present	6.5
[16]	Circular patch, cardboard	100 × 160	Cardboard	868 MHz	50	The design is simple but cannot be used universally as it is cardboard that changes its dielectric properties after coming into a moist environment	NA
Proposed antenna	Meandering technology and dipole	55 × 55	FR4	868	11	Design is simple	0.5

2. Details of Proposed Design

The major challenges for LoRa antennas are the requirements for small-diameter planar antennas that provide long-distance communication with better power management. In this section, the detailed antenna geometry is discussed, its equivalent circuit is presented, and the design strategy behind optimization is discussed. The designed structure was simulated in antenna simulator software, which is based on the FEM method.

2.1. Design Strategy. The technical design strategy for the proposed antenna is briefly described in this section. It is critical to determine the antenna type, material, and thickness before beginning the design process. Because of its excellent performance, the planar meander line antenna was prioritized, and FR4 epoxy substrate material was used to reduce the antenna's fabrication cost. After that, the appropriate electromagnetic (EM) software was chosen. The antenna is designed and simulated using version 15.0 of the high-frequency structure simulator (HFSS). Utilizing the transmission line model equations, the proposed antenna is constructed. After selecting the operating frequency and application for which the antenna is needed, the antenna is designed using a reverse analysis process. The decided dimension is optimized to the required frequency band. The first step is to select the antenna technology such as meandered or MIMO, fractal, or metamaterial, as per the available space on the Lora module or on-chip [32–35]. After that, the proposed antenna is designed, and the dimensions are described as a variable so that it will count for parametric study. The dimensions and design are modified based on the parametric results to achieve the required frequency band and antenna performance. The antenna is designed using the technical strategy depicted in Figure 2.

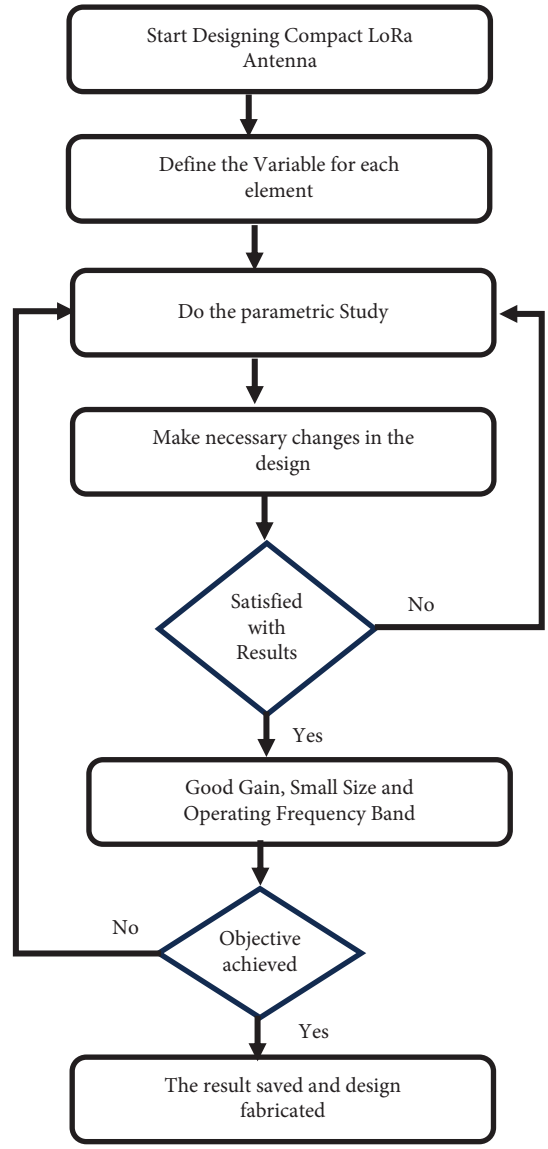

Figure 2: Flowchart for antenna designing strategy.

2.2. Antenna Geometry. The proposed meandered monopole antenna consists of the meandered monopole and dipole ground. The feed is provided using the rectangular stub between them. The proposed antenna's design is based on the coplanar waveguide (CPW) feed structure, which has been further enhanced through optimizations involving the dipole ground and rectangular monopole structures. These optimizations have led to the development of a meandering structure with a stub. The antenna is fabricated on a 1.6 mm thick FR4 substrate for mechanical support and as its foundation. The dimensions of the antenna have been carefully adjusted through a parametric study, resulting in an optimized size of $55\,\text{mm} \times 55\,\text{mm}$ ($0.16\lambda \times 0.16\lambda \times 0.005\lambda$). The design primarily comprises a folded meandered line, a dipole structure ground, and a stub for the feed.

The proposed antenna design dimensions are the following: $L = 55$ mm, $L_1 = 36$ mm, $L_2 = 22$ mm, $L_3 = 4$ mm, $L_4 = 47$ mm, $L_5 = 0.7$ mm, $W = 55$ mm, $W_1 = 0.8$, $W_2 = 8$ mm, $W_3 = 6$ mm, $W_4 = 11$ mm, $W_5 = 6.4$ mm, $W_6 = 4$ mm, $W_7 = 26$ mm, $W_8 = 0.4$ mm, $R = 3$ mm, and $r = 1$ mm. The proposed antenna has both the resonating patch and ground on the top of the substrate with stub as mentioned in Figures 3(a) and 3(b) showing the ground (green), patch (patch), and feed structure (black). In the parametric analysis, the meander structure has been examined, and the results are depicted in Figures 4 and 5. Figure 6 presents the S11(dB) graph, which demonstrates the impact of varying the feed line width on the antenna's performance. In addition, Figure 7 illustrates the S11(dB) graph, which showcases how changes in the length of the dipole structure influence the antenna's behavior. The −10 dB impedance bandwidth of the proposed antenna is 11 MHz from 860 to 871 MHz, which covers the LoRa spectrum. The gain for the complete band is more than 0.5 dB.

2.3. Meander Line Theory and Equivalent Circuit Diagram. An electrically small antenna is defined as an antenna whose maximum dimension is less than one-tenth of a wavelength [36]. A meander line antenna consists of standing and

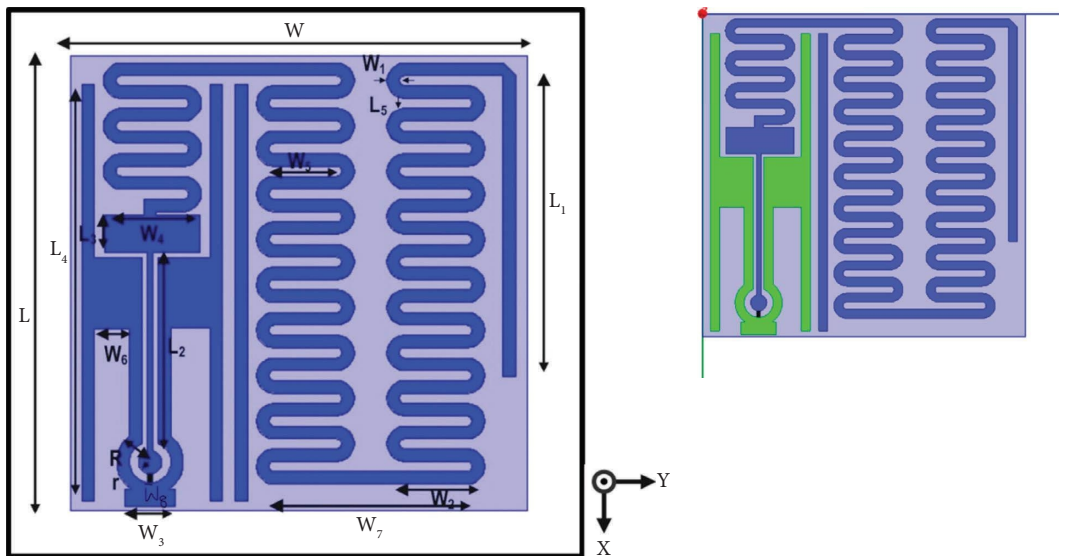

Figure 3: Configuration of the proposed LoRa antenna.

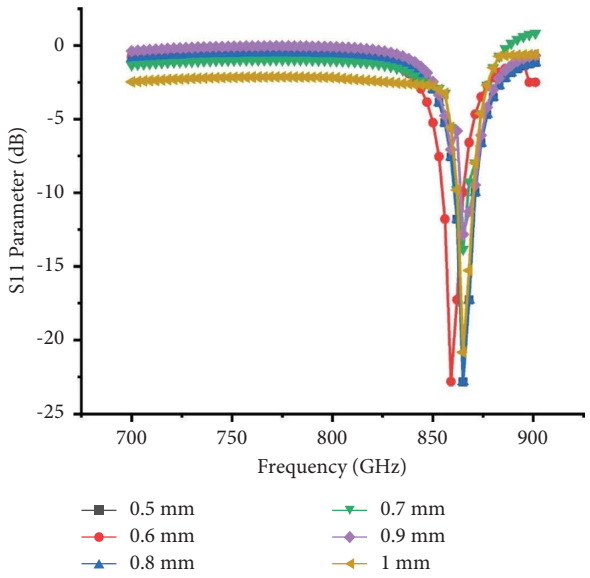

Figure 4: S11(dB) graph with the variation of the width of the meander (W_1).

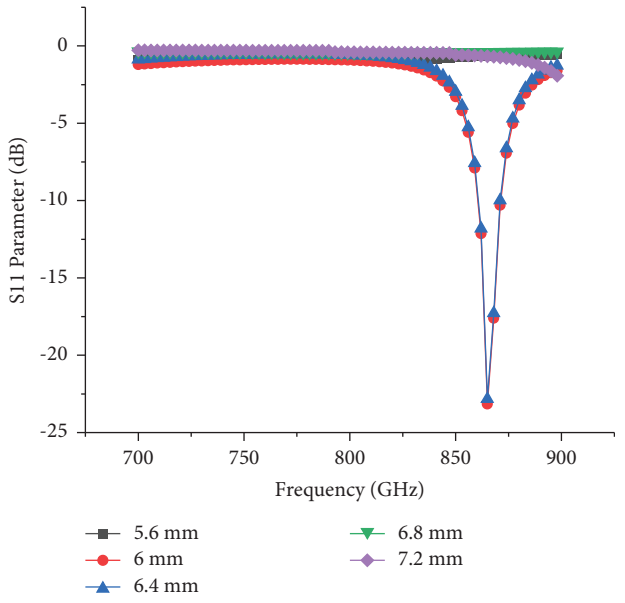

Figure 5: S11(dB) graph with a variation of length of meander (W_5).

sleeping lines; both lines together form a turn, and the number of turns helps increase the efficiency of the antenna. At the same meander, the split increases, and the resonance frequency decreases [37]. A spiral antenna is a development of the fundamental folding antenna and has frequencies significantly lower than single-element antenna resonances of identical length. The efficiency of meander line antennas surpasses that of traditional half and quarter-wavelength antennas. The effectiveness of these antennas relies on the reduction factor of their size, determined by the number of meandering elements per wavelength and the spacing between rectangular loops. In the proposed design, the spacing between the lines is set at 0.7 mm, while the width measures 0.8 mm. By ensuring smooth edges, the impedance matching and gain of the antenna are significantly enhanced. The meander line antenna consists of both vertical and horizontal components, each playing a distinct role. The vertical meander line functions as an inductor, while the horizontal one serves as a capacitor. A dipole patch antenna that behaves as ground typically consists of a conductive patch (often rectangular or circular) placed over a ground plane with a feedline connected to the patch. The equivalent circuit represents the antenna's impedance, resonance, and radiation characteristics. A meandered structure with two parallel stubs on both sides is a common configuration used in

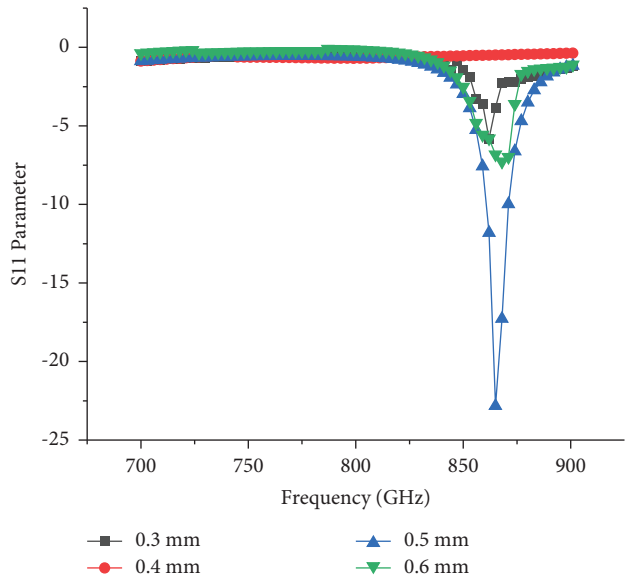

Figure 6: S11(dB) graph with the variation of the width of the feed line (W_8).

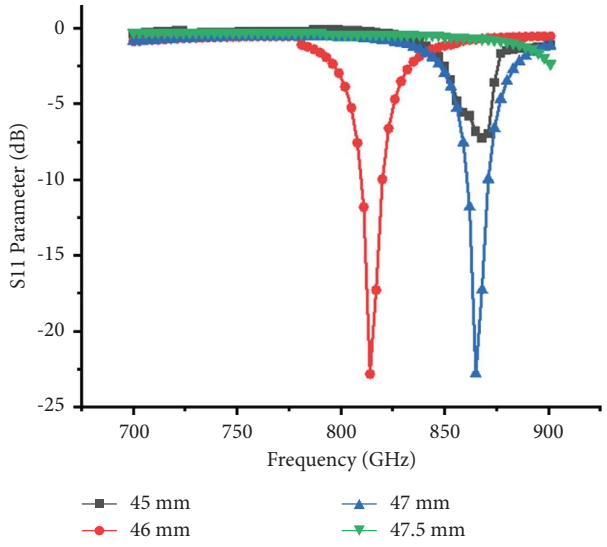

Figure 7: S11(dB) graph with the variation of length of a ground dipole (L_4).

microwave and RF (radio frequency) engineering for various applications, such as impedance matching, filtering, or tuning. To represent this structure with an equivalent circuit, a combination of lumped elements (resistors, capacitors, and inductors) is used to model its electrical behavior. Together, they contribute to the overall performance and characteristics of the antenna. By implementing the meander line design, the antenna achieves improved radiation efficiency compared to traditional half and quarter-wavelength antennas. This enhancement stems from the careful arrangement of the meandering elements and the optimization of the dimensions, specifically the spacing and width between the lines. The smooth edges play a crucial role in minimizing impedance mismatches, resulting in improved performance metrics, such as gain and radiation patterns.

Furthermore, the combination of the inductive and capacitive elements in the vertical and horizontal meander lines allows for better control over the antenna's electrical characteristics. This arrangement enables the antenna to effectively transmit and receive signals within the desired frequency range. The utilization of these elements ensures optimal utilization of the available space and enhances the overall performance of the antenna system. The proposed meander line antenna design offers enhanced radiation efficiency when compared to traditional half- and quarter-wavelength antennas. Through careful optimization of the meandering elements and dimensions, along with the utilization of inductive and capacitive components, the antenna achieves improved impedance matching, gain, and overall performance. The equivalent circuit diagram of the basic meander line is shown in Figure 8, where L and C are lumped elements. The equivalent circuit diagram of the proposed design is mentioned in Figure 9.

3. Simulations and Measurements Results

This section provides a detailed explanation of the fabricated antenna, along with the simulation and measurement results. In addition, the design includes the development of a connecting cable and the implementation of impedance-matching techniques. The effectiveness of impedance matching is primarily influenced by the width of the meandered line and ground plane. Figure 10 showcases the top 10(a) and bottom 10(b) of fabricated antennas. To assess the performance of the fabricated antenna, the S11(dB) parameters are measured using a network analyzer model number ZNLE6, as depicted in Figure 11. The return losses, both simulated and measured, are displayed in Figure 12. Notably, the antenna's bandwidth spans from 860 MHz to 871 MHz, encompassing the 868 MHz bands associated with LoRa technology.

Comparing the S11(dB) return loss graph to the simulated results, it is evident that they align closely. However, some variations in resonance may arise due to potential mismatches at the port connectors. The importance of impedance matching through the meandered line and ground plane width is emphasized. The figures included illustrating the simulated and fabricated antennas, as well as the measured S11(dB) parameters and return losses. The observed bandwidth of the antenna is confirmed to cover the desired LoRa frequency range. While the S11(dB) return loss closely matches the simulated results, slight variations in resonance are attributed to potential mismatching at the port connectors. The simulated gain band is also mentioned in Figure 13(a), which represents the copolarization and cross-polarisation band, gain at the operating band is more than 0.5 dB, and as mentioned in Figure 13(b), the efficiency of the proposed antenna is more than 75% for the complete operating band. Figure 14 shows the surface current on a radiating patch at 868 MHz. From the figure, it can be concluded that the surface current on a meandered line is opposite in direction and will cancel out to some extent, and

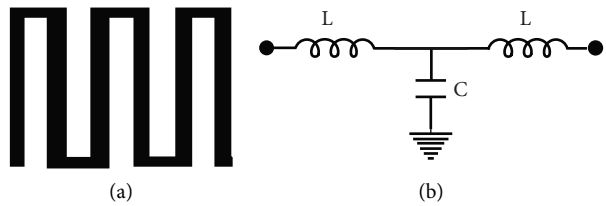

Figure 8: Basic meander line in figure (a) and its equivalent circuit diagram (b).

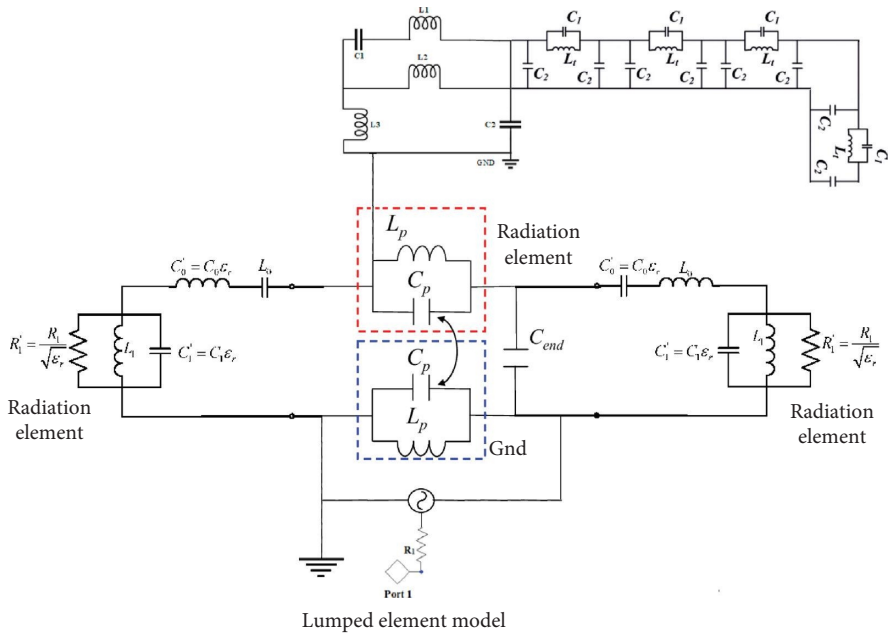

Figure 9: Equivalent electrical circuit of the proposed antenna.

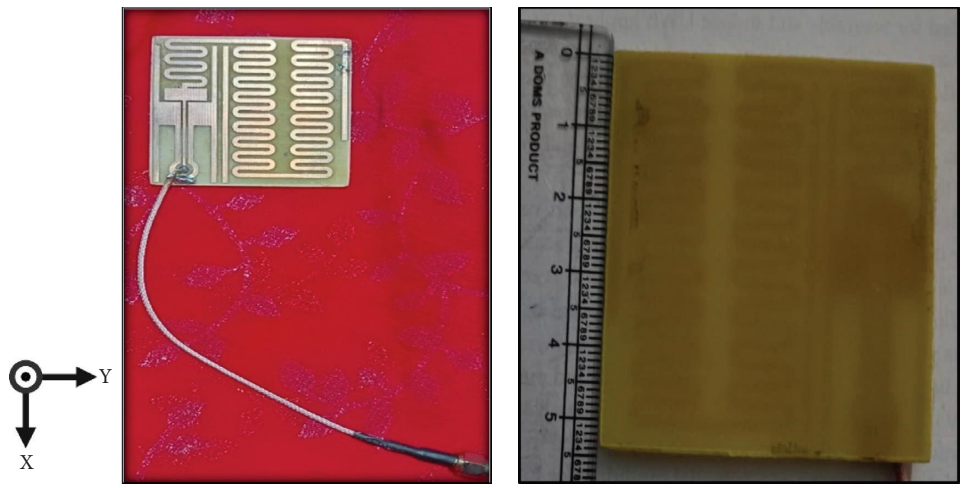

Figure 10: Snapshot of the fabricated antenna: (a) top and (b) bottom.

the resultant current will be at an angle of 36 degrees from the Y-axis, which can be verified by looking into the peak of the radiation pattern.

To validate the advantages of the newly developed antenna, a comparative analysis was conducted with an existing design operating in the same frequency band,

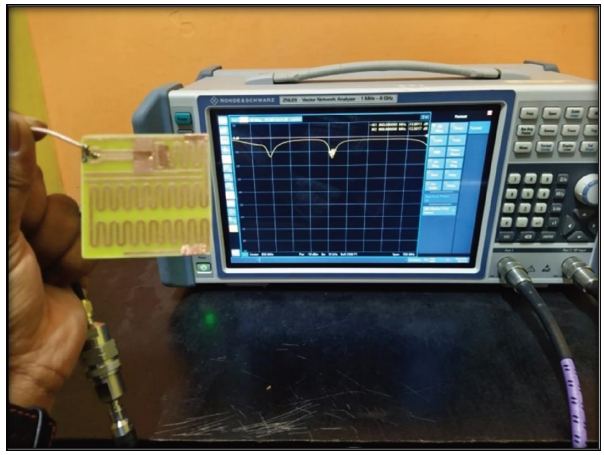

Figure 11: Fabricated antenna with vector network analyzer for S11(dB) measurement.

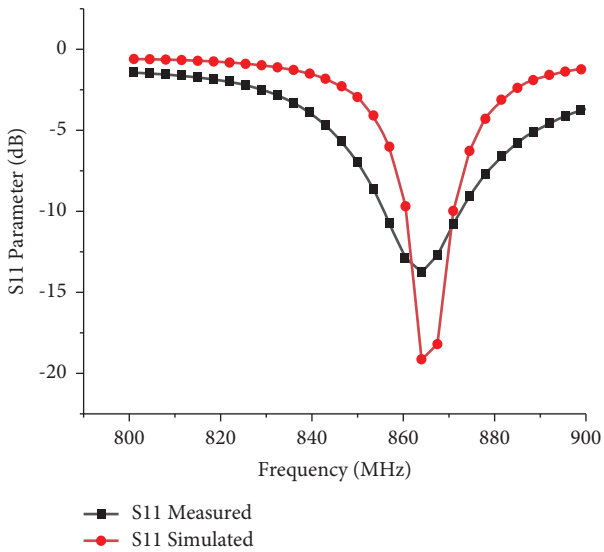

Figure 12: The simulated and measured S11(dB) graph (S11(dB) vs. frequency) of the proposed antenna.

specifically for LoRa applications. This comprehensive evaluation considered various parameters, including antenna dimensions, operating bands, bandwidth, radiation efficiency, gain, substrate material, and design complexity. The results of this comparison are tabulated in Table 1. One crucial aspect of the antenna's performance is its radiation pattern, which helps ascertain its directionality. To determine the gain of the proposed design accurately, a reference technique was employed. This involved placing the antenna, under test, in an anechoic chamber at a precise distance of 5.2 meters from a reference antenna, which was a ridge horn antenna. Figure 15 illustrates this anechoic chamber setup.

For the analysis, the radiation pattern was evaluated at a specific frequency of 868 MHz. The pattern was then characterized in both the E-plane and H-plane, which are depicted in Figure 16. The findings from the radiation pattern examination revealed that the maximum radiation occurred at an angle of 36 degrees in the theta plane. This phenomenon can be attributed to the direction in which the field is emitted from the antenna. Furthermore, the radiation pattern was effectively modeled using the designed antenna, as shown in Figure 17. The accuracy of this modeling process ensures that the antenna's behavior and performance can be predicted with reliability.

The proposed antenna's strengths were substantiated by conducting a thorough comparison with an existing design within the same frequency band and for LoRa applications. This analysis considered multiple critical factors, providing a comprehensive evaluation of the antenna's superiority. Moreover, the radiation pattern was studied in detail, enabling a precise understanding of the antenna's directionality and radiation characteristics. The gain measurement, achieved through the reference technique, contributed to the accurate assessment of the antenna's performance. The successful modeling of the radiation pattern with the designed antenna further reinforced the credibility of the study's outcomes. The meticulous evaluation and analysis undertaken throughout this study contribute significantly to the advancement of antenna technology and its applications in the field of wireless communication, particularly in LoRa-based systems operating in the 868 MHz frequency range.

4. Implementations

The final circuit design and assembled version can be seen in Figure 18, which depicts all pertinent components, including the proposed antenna, LoRa radio module, microcontroller, sensor antenna, and other passive components. Two sets are prepared so that one is used as a receiver and the other as a LoRa transmitter for the real-time LoRa connectivity experiments. The input signal is digital data using the Arduino module. The message was sent from transmitter to receiver and vice versa using Arduino software after traveling a certain distance in the different scenarios as mentioned in Section 4 of the manuscript. The maximum transmitted power is limited to 14 dBm. The radio module used is EByte E32-868T30S, SX1276, 868 MHz, 30 dBm, as shown in Figure 19. Therefore, a series of field experiments were conducted to evaluate the performance of a proposed antenna in different communication scenarios. The dimensions of the printed circuit board are 70 mm × 60 mm. The connection between the Arduino and the LoRa module is shown in Figure 20.

The antenna design has been effectively utilized with LoRa technology, enabling the transmission of data over considerable distances. In ideal conditions with a clear line of sight, the antenna achieved a remarkable communication range of up to 8 km. Even in urban settings, where obstacles and interference are more prevalent, it managed to maintain a reliable connection for distances exceeding 1 km. Moreover, within building areas, the antenna provided a satisfactory coverage of approximately 250 m. To validate its performance, the receiver was mounted on the roof of a vehicle on an express highway, while the transmitter was positioned in a line-of-sight environment. The communication remained

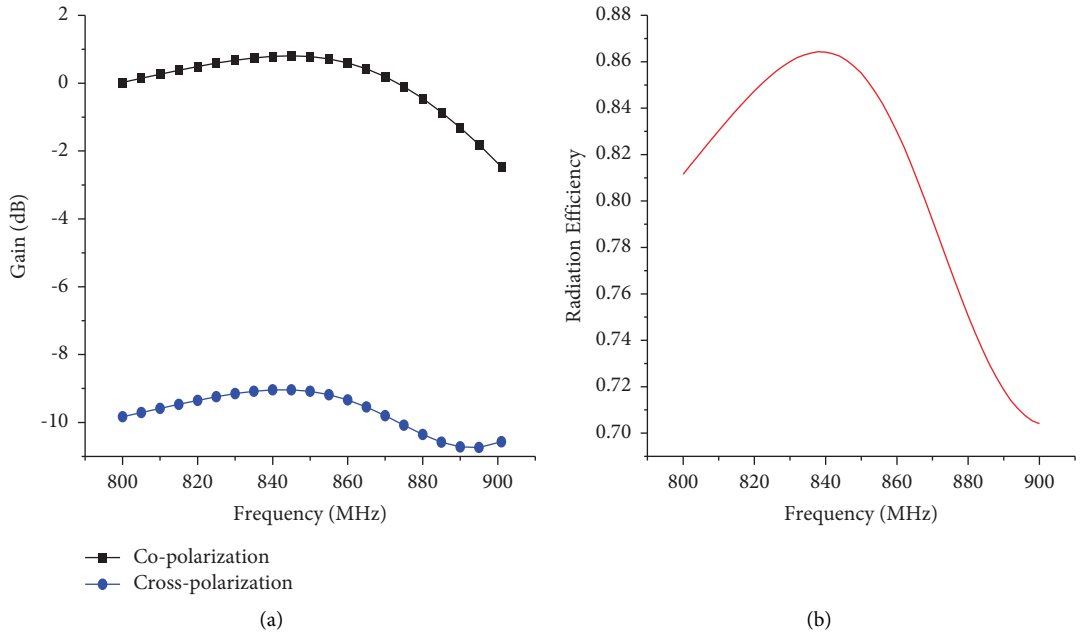

Figure 13: The simulated results: (a) gain vs. frequency graph of proposed antenna copolarization (black) and cross-polarization (blue) and (b) radiation efficiency vs. frequency band.

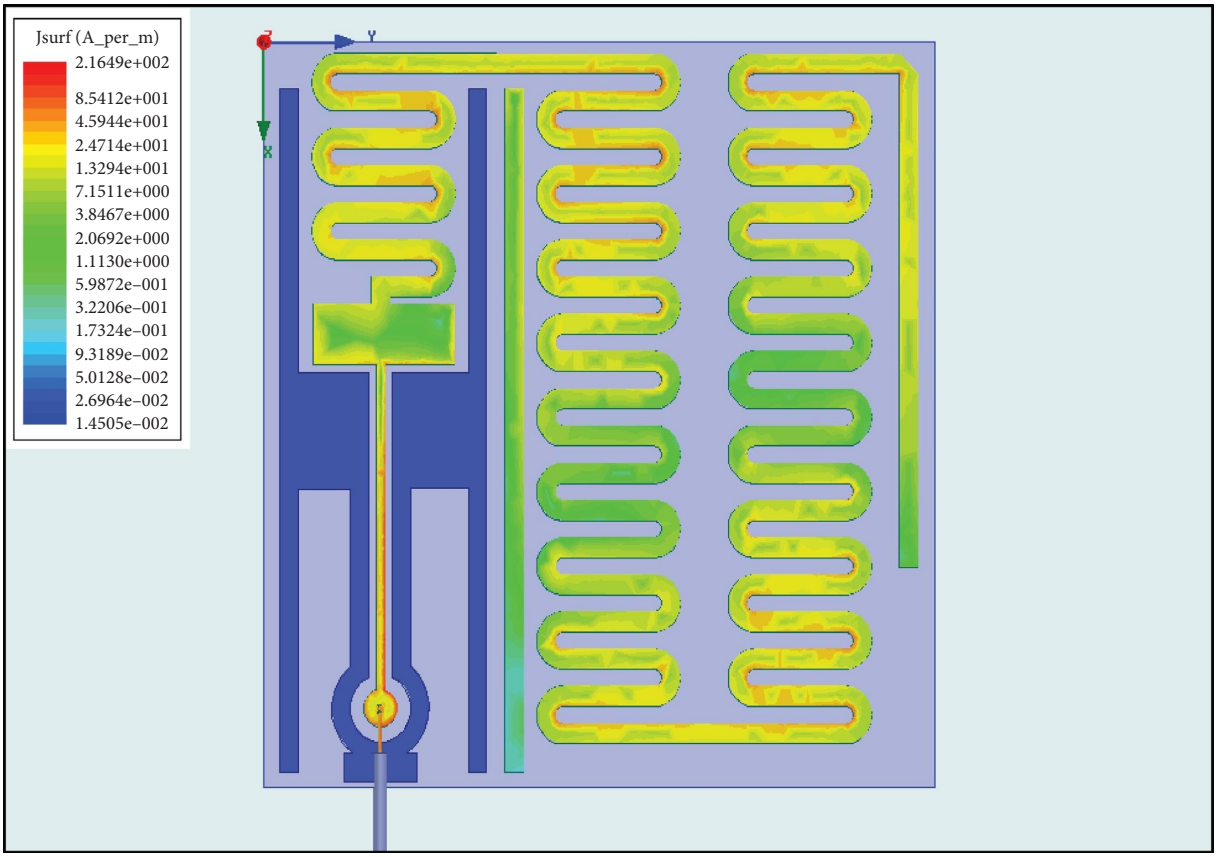

Figure 14: HFSS simulated profile for surface charge density on radiating patch at the frequency 868 MHz.

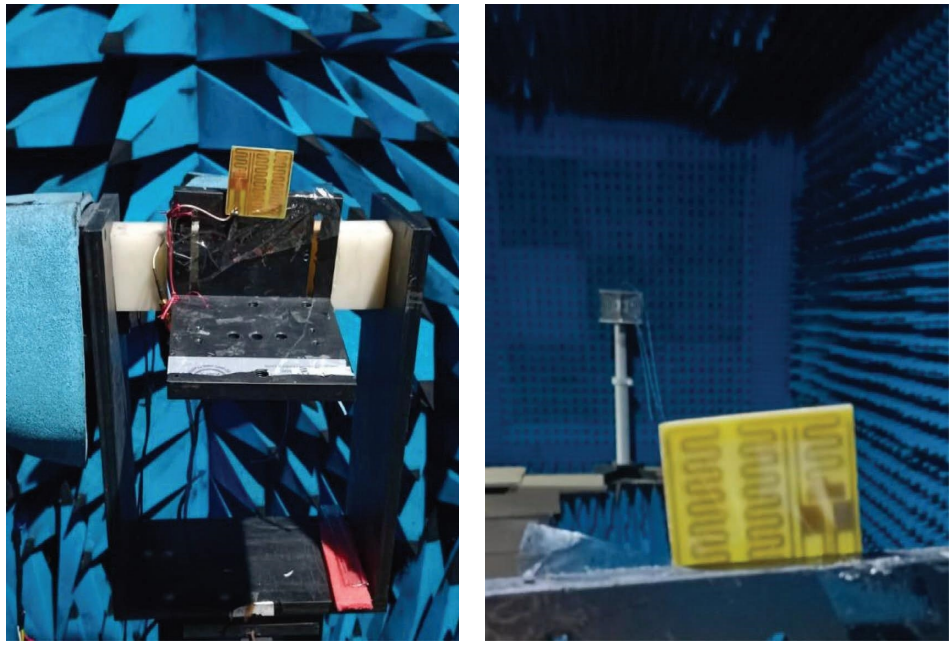

(a) (b)

Figure 15: The fabricated antenna is placed in an anechoic chamber for gain and pattern measurement: (a) the antenna is placed in an anechoic chamber and (b) horn and fabricated antenna at 5.2 m distance.

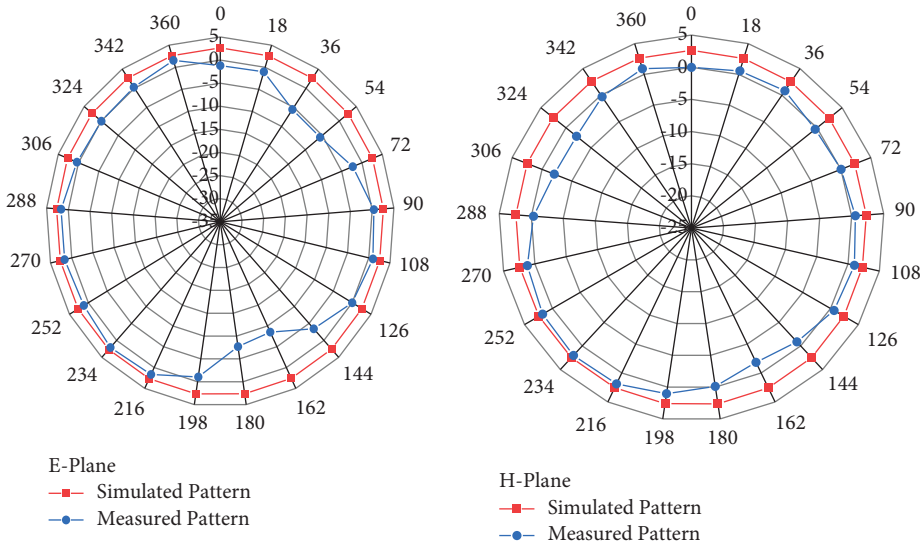

(a) (b)

Figure 16: The simulated and measured radiation pattern of the proposed antenna in (a) E-plane and (b) H-plane at 868 MHz.

consistently stable and connected over the entire 8 km range, as demonstrated in Figure 21.

Moving on to the second experiment, the receiver, equipped with a reference antenna, was placed on a vehicle, while the transmitter was located inside another moving car within an urban setting. The proposed antenna was used as the transmitter in this scenario, as illustrated in Figure 22. The results indicated that the communication range achieved with the proposed antenna was approximately 1.3 km. However, when the reference antenna was employed instead, the range was limited to only 900 m. This suggests that the proposed antenna provides superior coverage than the reference antenna.

In the third experiment, the transmitter was positioned on the balcony of a building, and the receiver antenna was moved to a neighboring building, as shown in Figure 23. Using the proposed antenna, the two LoRa devices were able to establish communication with each other within a range

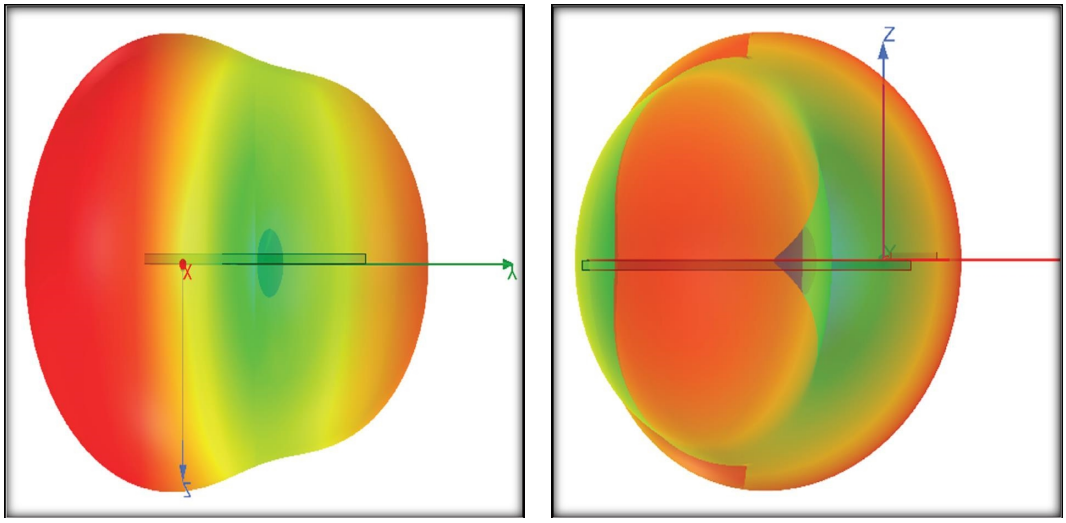

(a) (b)

Figure 17: The simulated radiation pattern modeled with the designed antenna: (a) E-plane view and (b) H-plane.

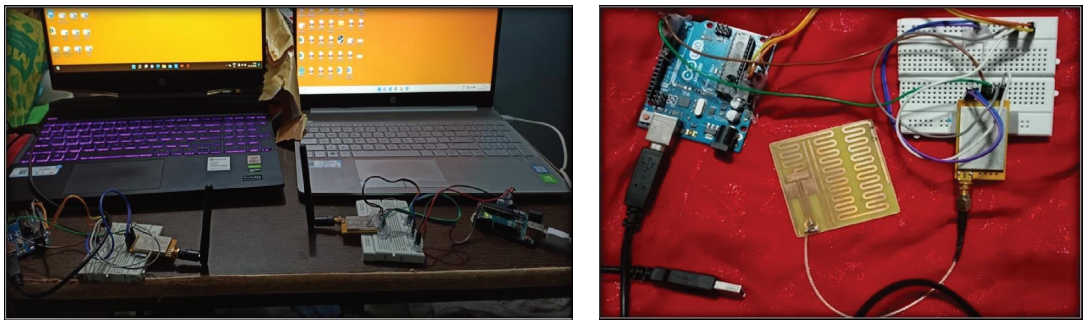

(a) (b)

Figure 18: Final circuit assembly with laptop, LoRa module, UNO R3 SMD Atmega328P board, jumping wires, and reference antenna (one is as transmitter and another one as receiver).

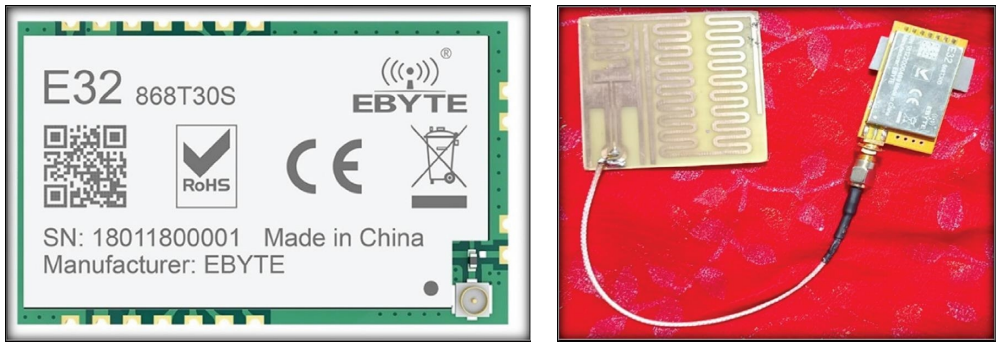

(a) (b)

Figure 19: The LoRa module (EByte E32-868T30S SX1276 868 MHz). (a) Module and (b) module with a proposed antenna.

of up to 250 m. On the other hand, when the reference antenna was used, the communication range was restricted to a maximum of 150 m.

To summarize, the conducted experiments assessed the performance of the proposed antenna in various scenarios. The first experiment demonstrated that the antenna facilitated well-connected communication over a distance of 8 km on an express highway. The second experiment revealed that the proposed antenna outperformed the reference antenna in an urban environment, achieving a communication range

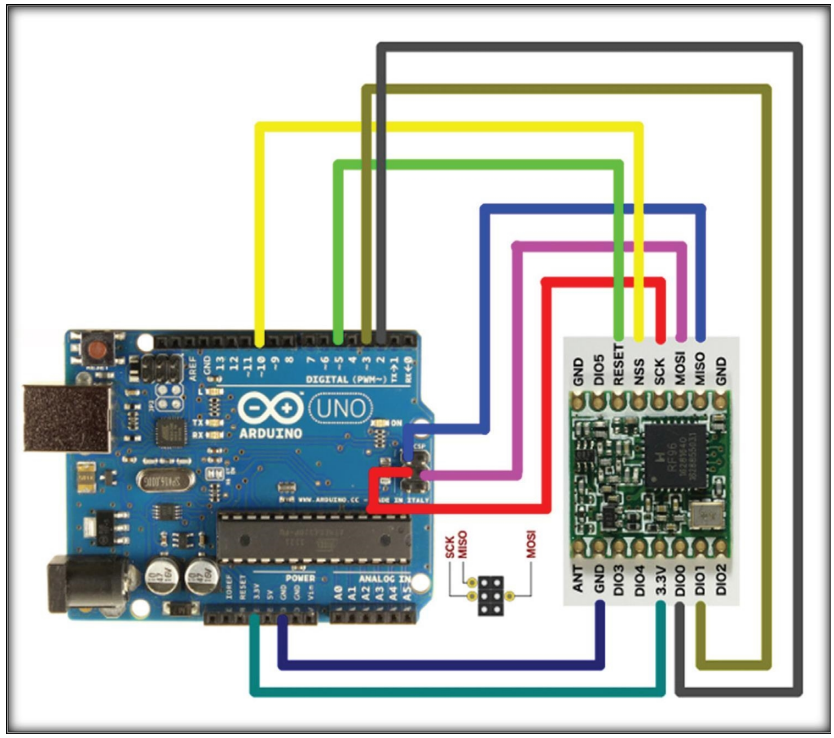

Figure 20: The connection between Arduino and LoRa module (868 MHz).

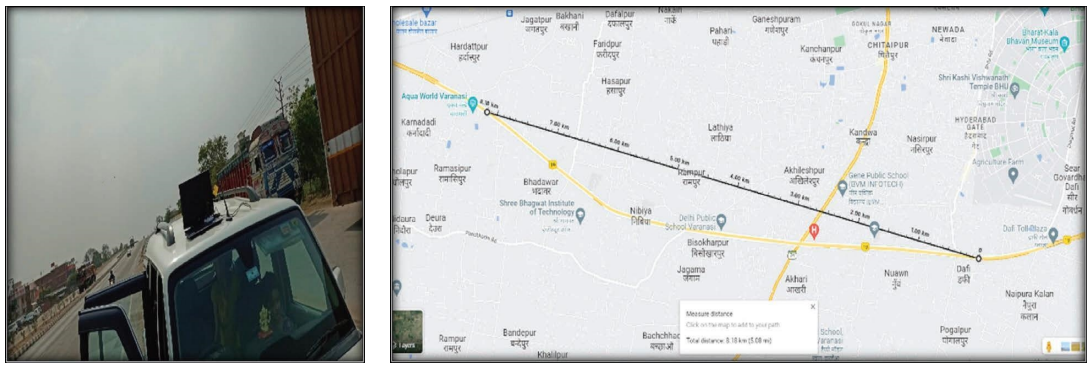

(a) (b)

Figure 21: First experiment-connectivity for line of sight: (a) receiver set up and (b) map where the experiment (Tx-transmitter and Rx-receiver) performed.

(a) (b)

Figure 22: Second experiment-connectivity in the urban environment: (a) receiver set up and (b) map where the experiment (Tx-transmitter and Rx-receiver) performed.

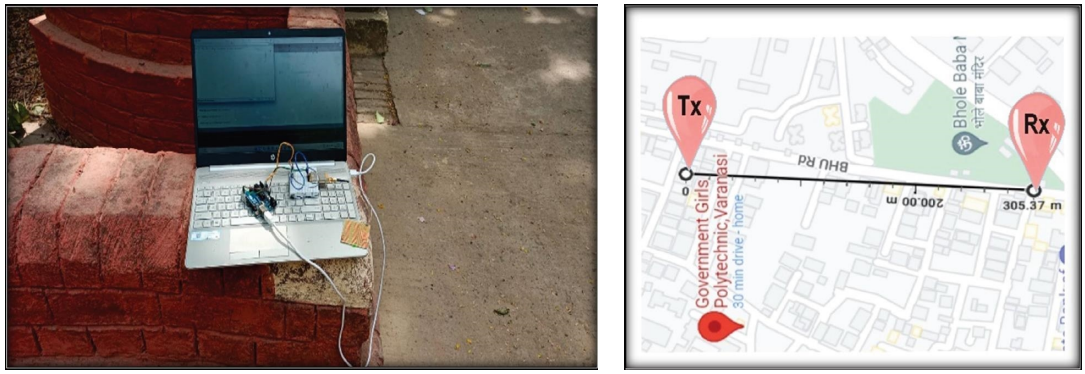

(a) (b)

Figure 23: Third experiment-setup for in-building connectivity: (a) receiver set up and (b) map where the experiment (Tx-transmitter and Rx-receiver) performed.

of 1.3 km compared to only 900 m. Lastly, the third experiment indicated that the proposed antenna enabled communication between two devices at a range of up to 250 m, surpassing the range of 150 m achieved with the reference antenna. These findings highlight the improved coverage capabilities of the proposed antenna in different real-world scenarios.

5. Conclusion

In this article, a meandered-dipole planar antenna is proposed for a long-range application, and the antenna is implemented in a real-time environment to verify its performance. The antenna latency is reported to be less than the standard monopole antenna used for LoRa module devices of the brand Arduino. The fabricated antenna results are in good agreement with the designed antenna. The achieved gain at the operating band is more than 0.5 dB and the efficiency of the proposed antenna is more than 75% for the complete operating band from 861 MHz to 871 MHz. The designed antenna is successfully implemented with LoRa connectivity and communicates the data up to 8 km in line-of-sight communication, more than 1 km in urban environments, and approximately 250 m of connectivity in building areas. The characteristics of the antenna were analyzed and found suitable for the LoRa applications. Future studies can focus on increasing the range of LoRa in high-traffic areas by adding more gateways along its route. The 433 MHz frequency can be combined with the LoRa antenna to make it multiband and universal in India. In this case, the LoRa antenna is only used to send data, but in the future, it could be used with many sensors to make the environment smarter, such as smart lighting or a smart agriculture system. The bandwidth can also be improved by adding meta surface ground structure to both antennas.

Data Availability

The data used to support the study are available from the corresponding author upon request.

Conflicts of Interest

The authors declare that they have no conflicts of interest.

Acknowledgments

Without my supervisor's assistance, this research project and article would not have been possible. We are inspired to work because of his expertise and enthusiasm for study. I want to express my gratitude to Professor M.K. Meshram and Researcher Rahul Dubey for their assistance and for providing the measuring facilities at IIT-BHU, Varanasi.

References

[1] M. Centenaro, L. Vangelista, A. Zanella, and M. Zorzi, "Long-range communications in unlicensed bands: the rising stars in the IoT and smart city scenarios," *IEEE Wireless Communications*, vol. 23, no. 5, pp. 60–67, 2016.

[2] R. S. Sinha, Y. Wei, and S.-H. Hwang, "A survey on lpwa technology: lora and nb-iot," *ICT Express*, vol. 3, 2017.

[3] ensembletech, "Ensemble tech private limited, g2, no. 21, srinivasa nagar rajiv gandhi salai chennai," 2012, https://www.ensembletech.in/lora-frequency-bands-india/.

[4] mokosmart, "How does lora sensor send and receive data," 2020, https://www.mokosmart.com/how-does-lora-sensor-send-and-receive-data/.

[5] P. Malik, S. Das, and S. Inthiyaz, "Long-range TechnologyEnabled smart communication: challenges and comparison," *Journal of Circuits, Systems, and Computers*, vol. 32, no. 10, 2022.

[6] T. J. Warnagiris and J. MinardoT, "Performance of a meandered line as an electrically small transmitting antennas Antenna and Propagation," *IEEE Transaction on*, vol. 46, 1998.

[7] Q. Zhang and Y. Gao, "Embedded Antenna Design on LoRa Radio for IoT Applications," in *Proceedings of the 12th European Conference on Antennas and Propagation (EuCAP 2018)*, p. 3, London, UK, April 2018.

[8] S. I. Lopes, F. Pereira, J. M. N. Vieira, N. B. Carvalho, and A. Curado, "Design of compact LoRa devices for smart building applications," in *Green Energy and Networking. GreeNets 2018*, J. Afonso, V. Monteiro, and J. Pinto, Eds., Springer, Berlin, Germany, 2019.

[9] A. Mushtaq, S. H. Gupta, and A. Rajawat, "Design and performance analysis of LoRa LPWAN antenna for IoT applications," in *Proceedings of the 2020 7th International Conference on Signal Processing and Integrated Networks (SPIN)*, pp. 1153–1156, Noida, India, February 2020.

[10] F. Ferrero and M. B. Toure, "Dual-band lora antenna: design and experiments," in *Proceedings of the 2019 IEEE Conference on Antenna Measurements & Applications (CAMA)*, pp. 243–246, Bali, Indonesia, October 2019.

[11] R. Hussain, S. I. Alhuwaimel, A. M. Algarni, K. Aljaloud, and N. Hussain, "A compact sub-GHz wide tunable antenna design for IoT applications," *Electronics*, vol. 11, no. 7, p. 1074, 2022.

[12] A. Dala and T. Arslan, "Design, implementation, and measurement procedure of underwater and water surface antenna for LoRa communication," *Sensors*, vol. 21, no. 4, p. 1337, 2021.

[13] C. Rohan, J. Audet, and A. Keating, "Small split-ring resonators as efficient antennas for remote LoRa IOT systems—a path to reduce physical interference," *Sensors*, vol. 21, no. 23, p. 7779, 2021.

[14] N. F. Ibrahim, P. A. Dzabletey, H. Kim, and J.-Y. Chung, "An all-textile dual-band antenna for BLE and LoRa wireless communications," *Electronics*, vol. 10, no. 23, p. 2967, 2021.

[15] X. Wang, L. Xing, and H. Wang, "A wearable textile antenna for lora applications," in *Proceedings of the 2021 IEEE 4th International Conference on Electronic Information and Communication Technology (ICEICT)*, pp. 613–615, Xi'an, China, August 2021.

[16] F. Mira, X. Artiga, I. Llamas-Garro, F. Vázquez-Gallego, and J. S. Velázquez-González, "Circularly polarized dual-band LoRa/GPS antenna for a UAV-assisted hazardous gas and aerosol sensor," *Micromachines*, vol. 12, no. 4, p. 377, 2021.

[17] J. Dong, X. Yu, and G. Hu, "Design of a compact quad-band slot antenna for integrated mobile devices," *International Journal of Antennas and Propagation*, vol. 2016, Article ID 3717681, 9 pages, 2016.

[18] A. Bekasiewicz and S. Koziel, "Compact UWB monopole antenna for Internet of things applications," *Electronics Letters*, vol. 52, no. 7, pp. 492–494, 2016.

[19] A. Romputtal and C. Phongcharoenpanich, "Iot-linked integrated NFC and dual-band UHF/2.45 GHz RFID reader antenna scheme," *IEEE Access*, vol. 7, pp. 177832–177843, 2019.

[20] M. Shahidul Islam, M. T. Islam, M. A. Ullah, G. Kok Beng, N. Amin, and N. Misran, "A modified meander line microstrip patch antenna with enhanced bandwidth for 2.4 GHz ISM-band Internet of Things (IoT) applications," *IEEE Access*, vol. 7, pp. 127850–127861, 2019.

[21] R. M. Bichara, F. A. Asadallah, J. Constantine, and M. Awad, "A folded miniaturized antenna for IoT devices," in *Proceedings of the 2018 IEEE Conference on Antenna Measurements & Applications (CAMA)*, pp. 1–3, Vasteras, Sweden, September 2018.

[22] P. M. Sneha, N. Bilandi, and A. Gupta, "Narrow band-IoT and long-range technology of IoT smart communication: designs and challenges," *Computers & Industrial Engineering*, vol. 108572, 2022.

[23] N. Hussain, A. Abbas, S. M. Park, S. Gyoon Park, and N. Kim, "A compact tri-band Antenna based on inverted L stubs for smart devices," *Computers, Materials & Continua*, vol. 70, no. 2, pp. 3321–3331, 2022.

[24] G. Leon, R. R. Boix, and F. Medina, "A comparison among different reduced-size resonant microstrip patches," *Microwave and Optical Technology Letters*, vol. 29, no. 3, pp. 143–146, 2001.

[25] V. F. Fusco, *Foundations of Antenna Theory and Techniques"*, Pearson Education Limited, Upper Saddle River, NJ, USA, 2005.

[26] M. Alibakhshi-Kenari, M. Naser-Moghadasi, R. Ali Sadeghzadeh, B. Singh Virdee, and E. Limiti, "New Compact antenna based on simplified CRLH-TL for UWB wireless communication systems," *International Journal of RF and Microwave Computer-Aided Engineering*, vol. 26, no. 3, pp. 217–225, 2016.

[27] T. Yamano, J. Itoh, and Y. Kim, "Fundamental characteristics of planar folded dipole antenna with a feed line," in *Proceedings of the IEEE International Symposium on Antennas & Propagation and USNC/URSI Meeting*, San Diego, CA, USA, July 2008.

[28] M. Alibakhshikenari, B. S. Virdee, P. Shukla et al., "Metamaterial-inspired antenna array for application in microwave breast imaging systems for tumor detection," *IEEE Access*, vol. 8, Article ID 174667, 2020.

[29] M. Zheng, H. Wang, and Y. Hao, "Internal hexa-band folded monopole/dipole/loop antenna with four resonances for mobile device," *IEEE Transactions on Antennas and Propagation*, vol. 60, no. 6, pp. 2880–2885, 2012.

[30] P. K. Malik, R. Sharma, and R. Singh, "Industrial internet of things and its applications in industry 4.0: state of the art," *Computer Communications*, vol. 12, 2020.

[31] P. Tiwari and P. K. Malik, "Design of UWB antenna for the 5G mobile communication applications: a review," in *Proceedings of the 2020 International Conference on Computation, Automation and Knowledge Management (ICCAKM)*, pp. 24–30, Dubai, United Arab Emirates, July 2020.

[32] A. Kaur and P. K. Malik, "Multiband elliptical patch fractal and defected ground structures microstrip patch antenna for wireless applications," *Progress in Electromagnetics Research B*, vol. 91, pp. 157–173, 2021.

[33] M. Alibakhshi-Kenari, M. Naser-Moghadasi, R. A. Sadeghzadeh, B. S. Virdee, and E. Limiti, "New CRLH-based planar slotted antennas with helical inductors for wireless communication systems, RF-circuits and microwave devices at UHF–SHF bands," *Wireless Personal Communications*, vol. 92, no. 3, pp. 1029–1038, 2017.

[34] Y. Yang, Q. Chu, and C. Mao, "Multiband MIMO antenna for GSM, DCS, and LTE indoor applications," *IEEE Antennas and Wireless Propagation Letters*, vol. 15, pp. 1573–1576, 2016.

[35] J. Dong, X. Yu, and L. Deng, "A decoupled multiband dual-antenna system for WWAN/LTE smartphone applications," *IEEE Antennas and Wireless Propagation Letters*, vol. 16, pp. 1528–1532, 2017.

[36] S. Zhang, K. Zhao, Z. Ying, and S. He, "Adaptive quad-element multi-wideband antenna array for user-effective LTE MIMO mobile terminals," *IEEE Transactions on Antennas and Propagation*, vol. 61, no. 8, pp. 4275–4283, 2013.

[37] S. R. Best and J. D. Morrow, "Limitations of inductive Circuit model representations of meander line antennas," in *Proceedings of the IEEE Antennas and Propagation Society International Symposium. Digest. Held in conjunction with: USNC/CNC/URSI North American Radio Sci. Meeting (Cat. No.03CH37450)*, Columbus, OH, USA, June 2003.